AD-A057 975 NAVAL OCEAN SYSTEMS CENTER SAN DIEGO CA F/G 4/1
MAGNETIC SUBSTORMS AND IONOSPHERIC STORMS. A MEASUREMENT NETWOR--ETC(U)
MAY 78 P E ARGO, J R HILL, I J ROTHMULLER

UNCLASSIFIED NOSC/TR-256 NL

1 OF 1
AD A057 975

END
DATE FILMED
10-78
DDC

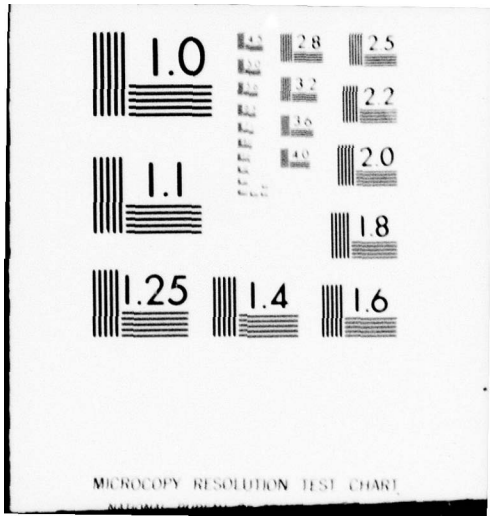
1.0
1.1
1.25
1.4
1.6
1.8
2.0
2.2
2.5
2.8
3.2
3.6
4.0
MICROCOPY RESOLUTION TEST CHART

LEVEL II

NOSC

NOSC TR 256

(14) NOSC/TR-256

Technical Report 256

(6)

MAGNETIC SUBSTORMS AND IONOSPHERIC STORMS.

A measurement network covering at least the entire Pacific area is seen as the key to the development of complete storm morphologies and a prediction capability.

(10) P.E. Argo, J.R. Hill, and I.J. Rothmuller

(11) 15 May 1978

(9) Interim Report. February 1976 – January 1978.

Prepared for
Naval Air Systems Command
and
Naval Environmental Prediction Research Facility

(12) 40 p.

(16) F52551

(17) ZF52551001

Approved for public release; distribution unlimited

NAVAL OCEAN SYSTEMS CENTER
SAN DIEGO, CALIFORNIA 92152

NAVAL OCEAN SYSTEMS CENTER, SAN DIEGO, CA 92152

AN ACTIVITY OF THE NAVAL MATERIAL COMMAND

RR GAVAZZI, CAPT USN
Commander

HL BLOOD
Technical Director

ADMINISTRATIVE INFORMATION

This study was made for the Naval Air Systems Command (AIR 370) and the Naval Environmental Prediction Research Facility by the Naval Ocean Systems Center, EM Propagation Division (Code 532), under project MP11, as part of an effort to develop earth environment disturbance forecasting techniques. The authors appreciate the help of MP Gannis in preparing the report. This work was performed between February 1976 and January 1978.

Released by
JH Richter, Head
EM Propagation
Division

Under authority of
JD Hightower, Head
Environmental Sciences
Department

UNCLASSIFIED

SECURITY CLASSIFICATION OF THIS PAGE (When Data Entered)

REPORT DOCUMENTATION PAGE		READ INSTRUCTIONS BEFORE COMPLETING FORM
1. REPORT NUMBER NOSC Technical Report 256 (TR 256)	2. GOVT ACCESSION NO.	3. RECIPIENT'S CATALOG NUMBER
4. TITLE (and Subtitle) MAGNETIC SUBSTORMS AND IONOSPHERIC STORMS A measurement network covering at least the entire Pacific area is seen as the key to the development of complete storm morphologies and a prediction capability.		5. TYPE OF REPORT & PERIOD COVERED Interim February 1976 through January 1978 6. PERFORMING ORG. REPORT NUMBER
7. AUTHOR(s) PE Argo, JR Hill, and IJ Rothmuller		8. CONTRACT OR GRANT NUMBER(s)
9. PERFORMING ORGANIZATION NAME AND ADDRESS Naval Ocean Systems Center San Diego, California 92152		10. PROGRAM ELEMENT, PROJECT, TASK AREA & WORK UNIT NUMBERS 62759N, F52551, ZF52551001, MP11
11. CONTROLLING OFFICE NAME AND ADDRESS Naval Air Systems Command and Naval Environmental Prediction Research Facility		12. REPORT DATE 15 May 1978 13. NUMBER OF PAGES 38
14. MONITORING AGENCY NAME & ADDRESS(if different from Controlling Office)		15. SECURITY CLASS. (of this report) Unclassified 15a. DECLASSIFICATION/DOWNGRADING SCHEDULE

16. DISTRIBUTION STATEMENT (of this Report)

Approved for public release; distribution unlimited

17. DISTRIBUTION STATEMENT (of the abstract entered in Block 20, if different from Report)

18. SUPPLEMENTARY NOTES

19. KEY WORDS (Continue on reverse side if necessary and identify by block number)

Disturbances – Magnetosphere
Disturbances – Propagation
Ionospheric disturbances
Propagation

20. ABSTRACT (Continue on reverse side if necessary and identify by block number)

Geomagnetic and ionospheric variations are extremely important to the Navy because many C^3 and surveillance systems depend upon the stability of the geomagnetic field and ionosphere for reliable operation. For example, rapid geomagnetic pulsations may obscure submarines from our ASW detectors, and ionospheric storm depletions or enhancements of the F-region may compromise covert Naval communications. To alleviate the damaging effects of these variations, a real-time environmental prediction/assessment system must be developed with inputs into a model describing effects of the variations on the system.

This report documents the present understanding of both magnetospheric substorms and ionospheric storms, and suggests a program to expedite the development of an operational model for Naval use. (continued)

DD FORM 1 JAN 73 1473 EDITION OF 1 NOV 65 IS OBSOLETE
S/N 0102-014-6601 |

UNCLASSIFIED

SECURITY CLASSIFICATION OF THIS PAGE (When Data Entered)

20. (continued)

Magnetospheric substorms appear to be the causative mechanism of the global ionospheric storm. A digest of the major models of magnetospheric substorms is presented in chapter 1. Chapter 2 discusses the ionospheric storms that are identified with magnetospheric substorms.

OBJECTIVE

Gather data on magnetospheric substorms, and the ensuing ionospheric storms with a view to the development of models useful in minimizing the detrimental impact of these processes on Naval communications.

RESULTS

1. The general morphology of both magnetospheric substorms and ionospheric storms has been documented, although much more study is necessary before any accurate modeling can be done.

2. A model of the "shock front" preceding some ionospheric storms has been developed.

RECOMMENDATIONS

Additional data, both magnetospheric and ionospheric, must be acquired before accurate and detailed models of these processes can be developed. Presently, a large-scale effort is being pointed this direction, in the International Magnetospheric Study (IMS).

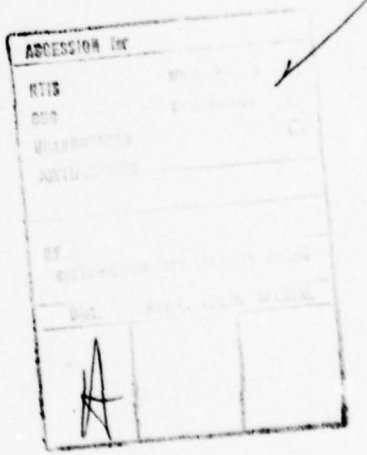

PREFACE

Geomagnetic and ionospheric variations are extremely important to the Navy because many C^3 and surveillance systems depend upon the stability of the geomagnetic field and ionosphere for reliable operation. For example, rapid geomagnetic pulsations may obscure submarines from our ASW detectors, and ionospheric storm depletions or enhancements of the F-region may compromise covert Naval communications. To alleviate the damaging effects of these variations, a real-time environmental prediction/assessment system must be developed with inputs into a model describing effects of the variations on the system.

This report documents the present understanding of both magnetospheric substorms and ionospheric storms, and suggests a program to expedite the development of an operational model for Naval use.

Magnetospheric substorms appear to be the causative mechanism of the global ionospheric storm. A digest of the major models of magnetospheric substorms is presented in chapter 1. Chapter 2 discusses the ionospheric storms that are identified with magnetospheric substorms.

CONTENTS

CHAPTER 1: MAGNETOSPHERIC SUBSTORMS

INTRODUCTION

The solar wind (a neutral plasma) flowing by and interacting with the earth's magnetic field undergoes charge separation. Thus, the mechanical energy of the solar wind is converted to an electric potential by the geomagnetic field in a dynamo-like manner. Akasofu (1975)* estimates that the solar wind is putting energy into the magnetosphere at the rate of $\sim 10^{19}$ erg/s.** Assuming that the magnetosphere cannot hold an infinite amount of energy, we might expect some mechanism for energy release. A magnetospheric substorm is an *implosive* release of this magnetospherically stored energy into the polar ionosphere, and can be viewed as a form of capacitive discharge through a current system to be described later.

The energy release (or conversion of potential energy into mechanical energy) is manifested through many forms in the polar ionosphere, as documented by Akasofu (1968):***

Auroral substorm. Greatly enhanced auroral activity – specific patterns of variation

Polar magnetic substorm. Enhanced auroral electrojet, creating magnetic disturbances

Ionospheric substorm. Anomalous ionization and heating in lower ionosphere by auroral particles, generating traveling wave disturbances and infrasonic waves – resulting in major changes in circulation

X-ray substorm. Bremsstrahlung from energetic precipitated electrons

Proton aurora substorm. Precipitating low-energy protons enhance auroral luminosity in the Balmer lines

Vlf emission substorm. Hiss and chorus coming from precipitated particles

Micropulsation substorm. Ulf electromagnetic waves, thought to be of magnetospheric origin and propagated as hydromagnetic waves

Axford (1969)**** has estimated the magnitude of three forms of energy dissipated during a geomagnetic substorm to be:

1. $\sim 10^{18}$ erg/s from production of aurora
2. Joule heating (current) of polar ionosphere $\sim 10^{18}$ erg/s
3. Ring current $10^{18} - 10^{19}$ erg/s

---

*Akasofu, SI, "The solar wind – magnetosphere dynamo and the magnetospheric substorm," Planet Space Sci, 23, 817, 1975

**1 erg/s = 0.1 μW

***Akasofu, SI, "Polar and magnetospheric substorms," Springer Verlag, 1968

****Axford, I, "Magnetospheric convection," Rev of Geophys, 7, 921, 1969

It can be seen that the total rate of energy release is on the order of the energy input – indicating that substorms must be frequent phenomena, assuming substorms are the major release form.

Each substorm injects protons into the trapping or radiation belt. The adiabatic motion of these protons around the earth forms what is called a "ring current." If there has not been another substorm within 6 hours, most of the protons will have been lost from the ring current. However, successive substorms at intervals of 2–3 hours will accumulate protons in a very intense ring current (see fig 1). The effect of this ring current is such that its magnetic field opposes the normal geomagnetic field, and so, at low latitudes, there will be a ground-level geomagnetic field decrease – called a "geomagnetic storm." The development of the intense ring current through the series of magnetospheric substorms occurring

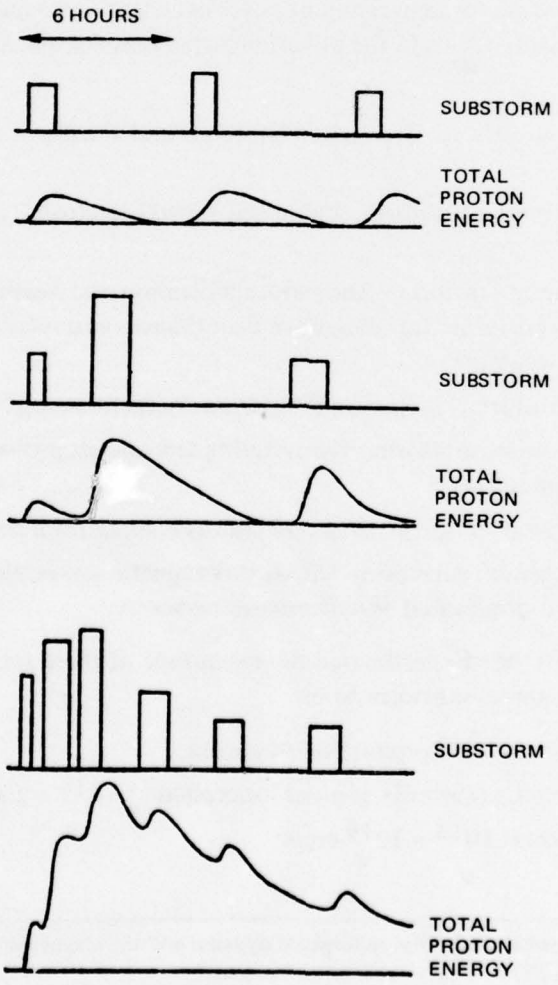

Figure 1. Relationship between substorm occurrence frequency and "trapped" proton population in the ring current.

back to back is commonly called a *magnetospheric storm*, of which the geomagnetic storm is one manifestation.

The rest of this report covers in detail the phenomena of magnetospheric substorms. Succeeding sections provide a refresher on magnetospheric configuration and morphology; deal with the phenomenology of the "normal" substorm; give some experimental observations during substorms; and examine some of the present areas of conflict in the interpretations of the physics of substorms.

MAGNETOSPHERIC CONFIGURATION AND MORPHOLOGY

The solar wind is a plasma streaming radially outward from the sun, with a weak magnetic field imbedded. Because the proton gyro radius is on the order of 100 km (near the earth), the earth's dipolar magnetic field acts as an obstacle to the solar wind flow in a basically hydrodynamic interaction. The following descriptions are depicted in figures 2 and 3.

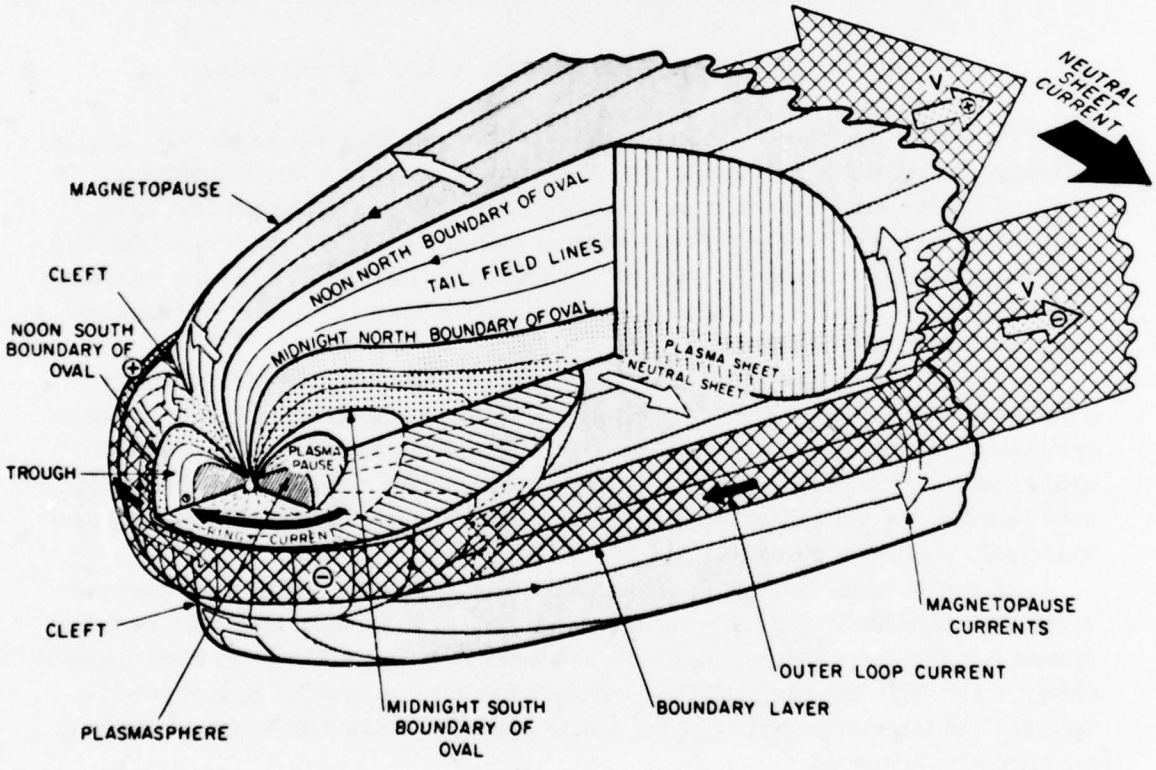

Figure 2. The magnetosphere.

Because the earth's dipolar magnetic pressure falls off as r^{-6}, at some point the solar wind pressure (p) dominates the earth's magnetic pressure (ie, $p > B^2/2\mu_o$) – this is the solar wind region. Closer to the earth, the geomagnetic pressure dominates ($p < B^2/2\mu_o$) and we

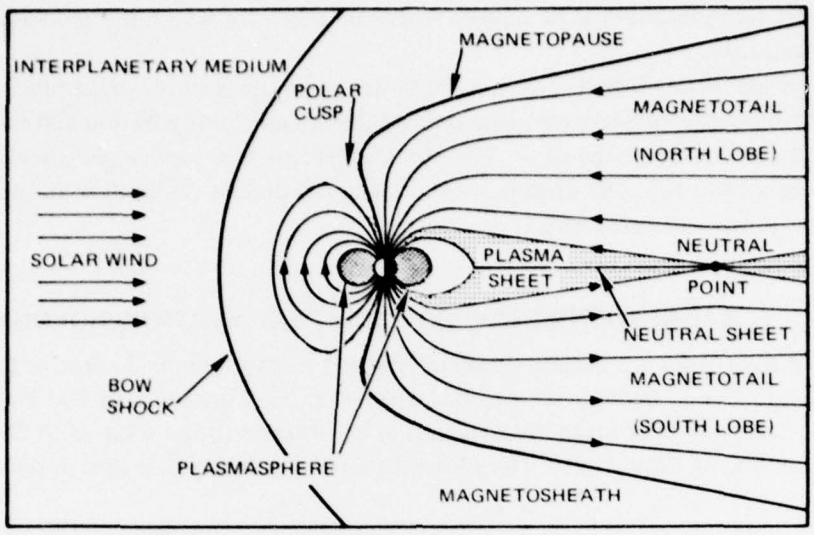

Figure 3. Magnetosphere, showing magnetic configuration and bowshock.

are in the magnetosphere. The boundary between these conditions (where $p \approx B^2/2\mu_o$) is called the *magnetopause*, and moves with changes in the dynamic solar wind pressure.

The solar wind is supersonic (specifically, super Alfvenic) and, therefore, a *shock front* must develop in front of the magnetopause (see fig 3). Between the shock front and the magnetopause is a region of "shocked" interplanetary plasma called the *magnetosheath*. In this region are "scrambled" magnetic field lines, which must finally obey the magnetopause boundary condition that B_{normal} disappear.

The supersonic flow also ensures that a cavity of extremely low plasma density develops behind the earth. The cavity behind the earth, caused by the fluid flow, is not an open cavity because of the isotropic thermal pressure tending to close it. This *magnetospheric tail* is complicated, and cannot be explained by simple hydrodynamic theory. It must be treated as current sheets and changing magnetic fields. The tail field lines connect to the polar regions on the earth.

A way to understand the dynamics of the magnetosphere is to use the concept of merging (reconnection) of B fields imbedded in plasmas. As the inner field lines are being pressed together, they reconnect to form a new pair (fig 4), in an attempt to lower the total energy in the field. The plasma at the reconnection point (the so-called neutral point) is squeezed and accelerated away from the neutral point. The exact reconnection process is as yet poorly understood.

The major neutral point in the magnetosphere occurs where the interplanetary field merges with the dayside outermost closed terrestrial lines (fig 5). The motion of the solar wind then "drags" these lines back into the magnetotail. A southward interplanetary magnetic field (IMF) will cause enhanced merging at the front. That a northward IMF can have merging is one of the subtleties of the merging theory, because the fields are not strictly in antialignment. The effect of the southward IMF is that more field lines are moved across into the tail in a given time, causing an expansion of the polar cap/auroral oval, as well as

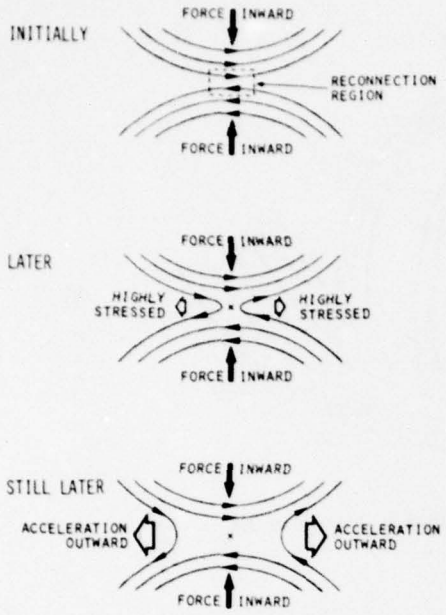

Figure 4. Diagrammatic interpretation of the reconnection process at an X-type neutral point.

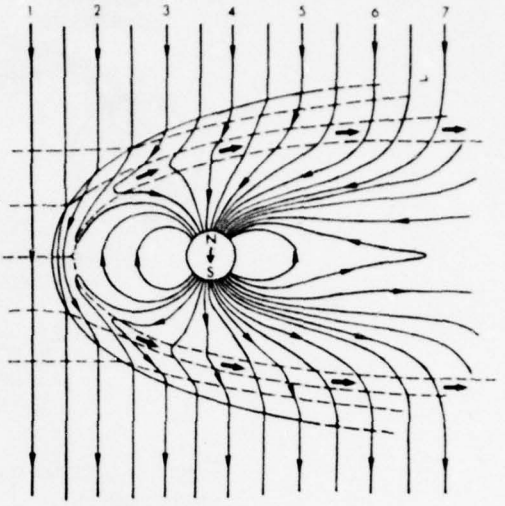

Figure 5. Magnetic field line motion due to merging at the nose, and the motion of the solar wind.

an equatorward motion of the noon cleft (the funnel-shaped connection between the magnetosheath and the earth, fig 6).

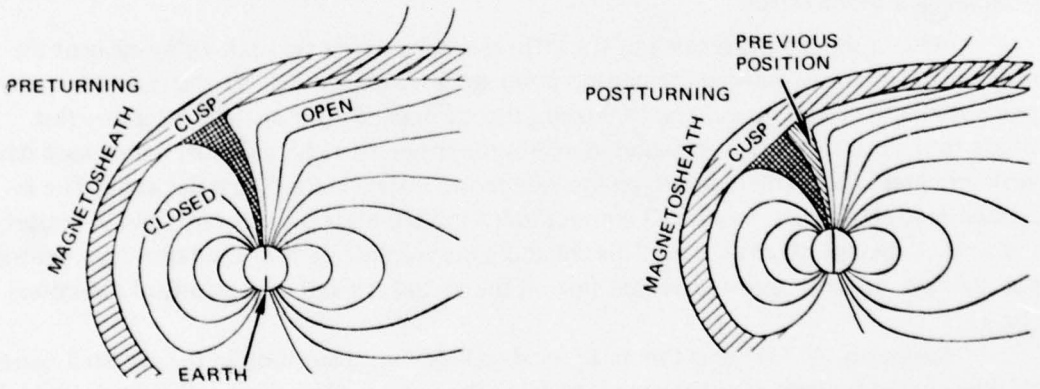

Figure 6. Equatorward motion of the polar cusp (cleft) due to southward turning of the IMF.

The increased density of field lines in the tail may also cause merging there – far down the tail (>50 R_E). This tail merging will be a slow, quasi-adiabatic effect, not the rapid substorm-caused merging to be examined later.

The solar wind "blowing" across the open field lines (polar) gives a $V_{\text{solar wind}} \times B_n$ electric field, yielding a 40–50-kV potential across the dawn-dusk magnetotail. This action can be viewed as a dynamo, with a resulting "crosstail" current flowing (fig 7). Because of

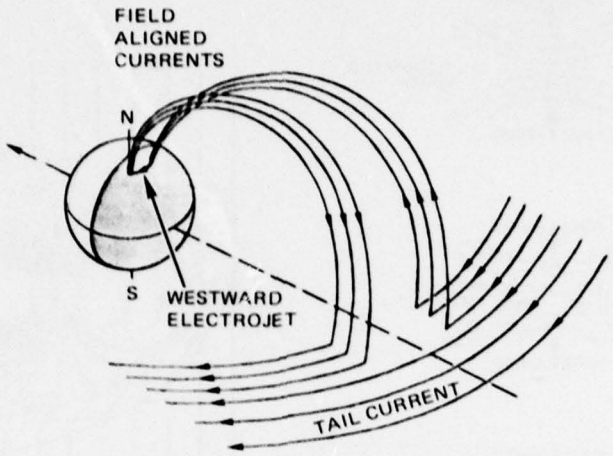

Figure 7. Crosstail and field aligned currents in the magnetosphere.

large conductivities in the nightside auroral oval, there may be slight leakage currents (field aligned) through the auroral zone.

SUBSTORMS

CLASSICAL SUBSTORM

After a southward turning of the IMF, there is an increased rate of merging at the magnetospheric nose, causing the neutral point to move earthward. At the same time, the polar cusp moves equatorward and the auroral zone expands (fig 6). The magnetic flux added to the tail from the solar wind increases the magnetic field, causing an increased dawn/dusk crosstail E-field (there is also an increase in the E-field across the polar cap). The increased tail E-field causes an E x B convection of the tail plasma earthward, which creates a thinning of the tail plasma sheet. This enhances the reconnection of the tail x-type neutral point which, in turn, causes increased flow in the earthward and antiearthward directions (fig 8).

Svalgaard (1973)* sees this as a "local collapse" or disruption in the crosstail current because suddenly there are no particles to carry the current. Hence, the disrupted crosstail manifests itself in a new circuit: from the dawn side magnetotail down the field to the dawn side of the oval, around the nightside oval (and over the polar cap), finally in field-aligned flow up to the dusk side tail (fig 7).

* Svalgaard, L, "Geomagnetic responses to the solar wind and solar activity," Stanford University, Institute for Plasma Research, Rept 555, 1973

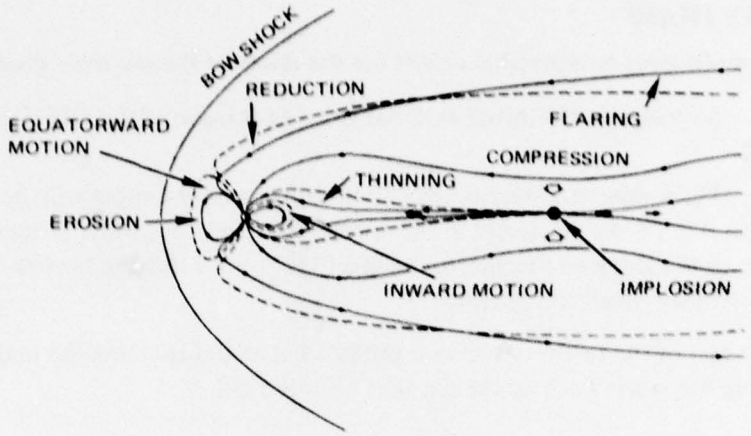

Figure 8. Changes in the magnetospheric configuration due to southward turning of the IMF.

Akasofu (1970)* has a different view of the triggering mechanism, with the following time sequence:

1. The increased crosstail potential causes increased current flow through the auroral circuit.

2. The increased field-aligned current flow passes some threshold, allowing sudden enhancement in anomalous resistivity along a field line (Akasofu suggests an ion-acoustic wave mechanism, by which energy is taken from the particle flow and converted to acoustic energy).

3. The potential drop along the field line increases, causing

4. Acceleration of auroral particles down field line (E-field), creating

5. Increased E-region ionization resulting in enhanced conductivity in the auroral zone.

6. The enhanced polar circuit conductivity acts as a short circuit to the magnetospheric dynamo and disrupts the crosstail current, causing

7. Further increases in polar circuit current, which in turn

8. Increases the production of ion-acoustic waves, maintaining potential drop along field line (maybe even increasing it) so more particles are accelerated, creating higher conductivity in the auroral E-region, with the cycle from 5–8 developing in a positive feedback mechanism.

Akasofu states that the short-circuiting of part of the magnetotail current (through the ionosphere) will cause the formation of a new neutral point at the weakened location in the magnetotail. Notice that the current flow from the dawn side to dusk is really manifested by electrons flowing the other direction; ie, streaming down the nightside field lines.

* Akasofu, SI, "Magnetospheric substorms: a model," Solar Terrestrial Physics/1970, part III, p 131–151, Oxford Press, 1972

RECOVERY PHASE

Akasofu gives two possible causes for the onset of the recovery phase:

1. A change in the initial external stress (a turning of the IMF from southward to northward).

2. The ionosphere may be able to hold stress only temporarily because a neutral wind is generated by the electrojet in the auroral E-region; and when the speed becomes comparable to the E-region ion speed, the electrojet ceases flowing because of a $V_n \times B$ potential resisting the electrojet motion.

The rest of the recovery phase is the process of transporting the magnetic flux produced during the storm back to the dayside from the tail.

RING CURRENT AND TRAPPED PARTICLES

Many of the particles accelerated earthward by the tail neutral point find themselves on "closed" geomagnetic field lines and, once there, cannot easily diffuse across the closed lines. The particles in the "trapping zone" undergo drifts around the earth (fig 9) caused by the curvature and gradients in the earth's magnetic field. The electrons move towards the dawn side (eastward) while protons drift towards evening (westward), constituting a net westward *ring current* in the trapping zone. The trapped electrons have the same energy (hence, greater velocity) that the trapped protons have (they have undergone the same accelerative forces in the tail neutral point) and, therefore, display a steeper pitch angle distribution; ie, the field-aligned momentum is greater. This means they penetrate deeper into the atmosphere and are more likely to undergo collisions that scatter them out of the "trapped" population. Therefore, mainly protons are left in the ring current, and because these protons have drifted to the evening sector, there remains a net asymmetry in the ring current.

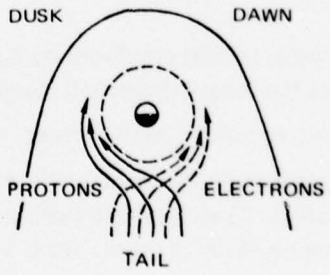

Figure 9. Development of the ring current.

OBSERVATIONS OF SUBSTORM ACTIVITY

AURORAL ACTIVITY

The close relationship between auroral displays and geomagnetic disturbances has been recognized since 1950. Akasofu (1968) compared aurora to the cathode-ray tube; ie, the fluorescent display as the screen is bombarded by the electron beam. The aurora are large-scale phenomena with complicated spatial features that vary in time. Each observing station travels through the aurora as the earth rotates, making it difficult to understand the auroral morphology without the use of all-sky camera chains *and* polar satellites. Akasofu (1964)* has developed a schematic chain of events:

1.	T=0	quiet	(fig 10A)
2.	T=0–5	min	brightening of the quiet midnight arc (fig 10B)
3.	T=5–10	min	poleward motion of the brightened arc, trailing "breakup" (bulge effect) (fig 10C)
4.	T=10–30	min	bulge expands – mainly through a westward traveling surge (fig 10D)
5.	T=30 min–1 h		recovery stage: contraction of the poleward bulge (fig 10E)

The initial poleward motion of the aurora (step 3) can be explained by the action of enhanced reconnection in the tail (fig 11), because auroras tend to appear on the poleward edge of the close field lines. The westward traveling surge seen in the aurora (step 4) is caused by an influx of energetic electrons – the auroral motion is a manifestation of the westward motion of the particle dumping region. Later in this report, in examining Akasofu's models (fig 13), the substorm cause of the westward motion will be pointed out.

SATELLITE MEASUREMENTS

Satellite measurements have given a picture of the magnetospheric configuration during substorms. There are basic problems in interpreting the information, however, because it is still difficult to separate space and time variations.

During the storm onset there is plasma motion in the tail, indicating a thinning of the plasma sheet and earthward motion of the trapping regions (see fig 8). This occurs because the increased convection causes a tail E-field pinch. The geomagnetic field configuration at 6–10 R_E becomes more dipole-like – coinciding with westward electrojet in the auroral region. This increased activity causes the injection of plasma into the trapping regions from the tail regions.

SUBSTORM-RELATED CURRENT SYSTEMS

Chapman and Birkeland in 1910 developed "equivalent current" systems to describe ground magnetic fluctuations, in which they observed the need for an auroral electrojet

*Akasofu, SI, "The development of the auroral substorm," Plant Space Sci, 12, 273, 1964

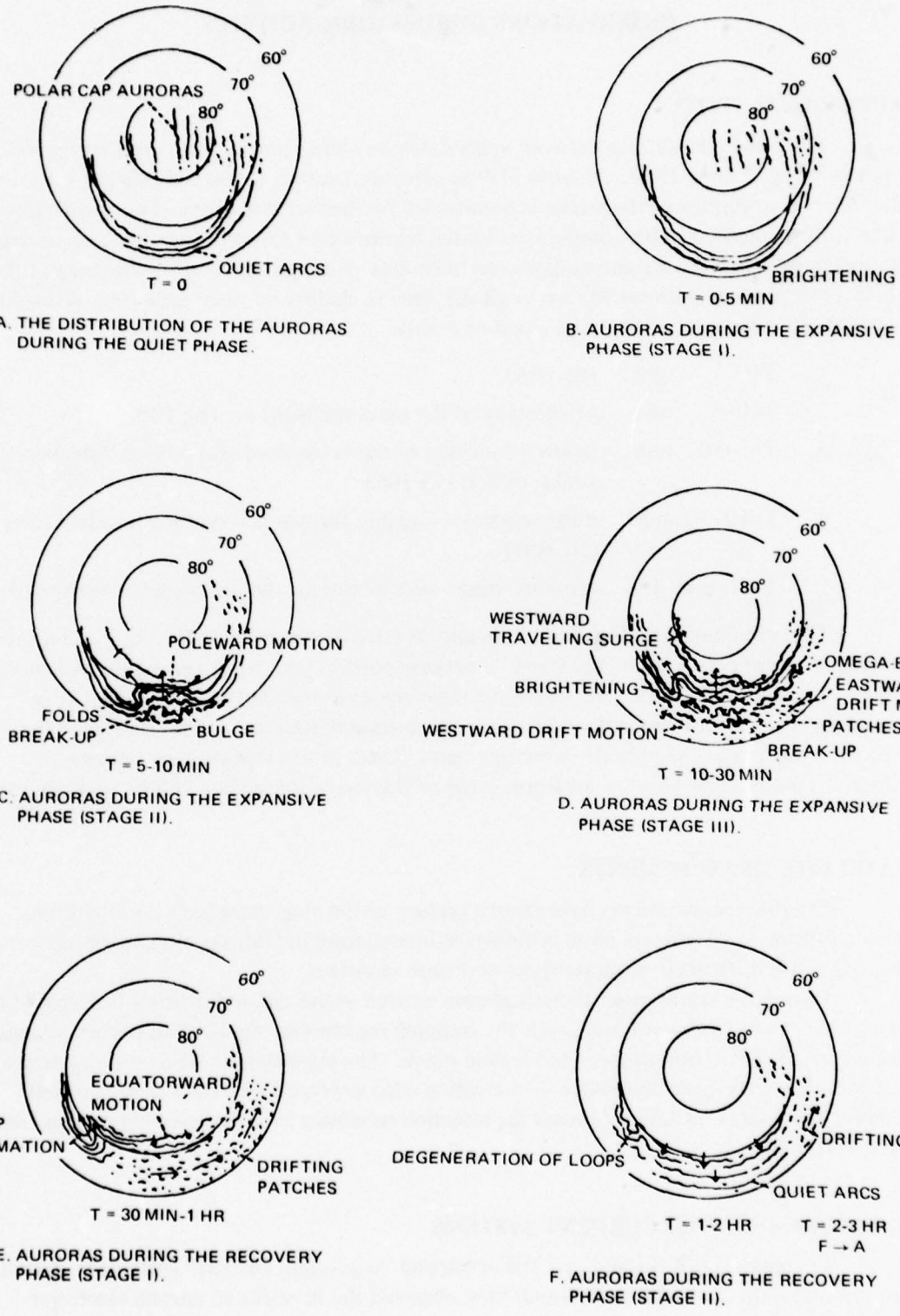

Figure 10. Development of the auroral substorm (Akasofu, 1964, reprinted with permission).

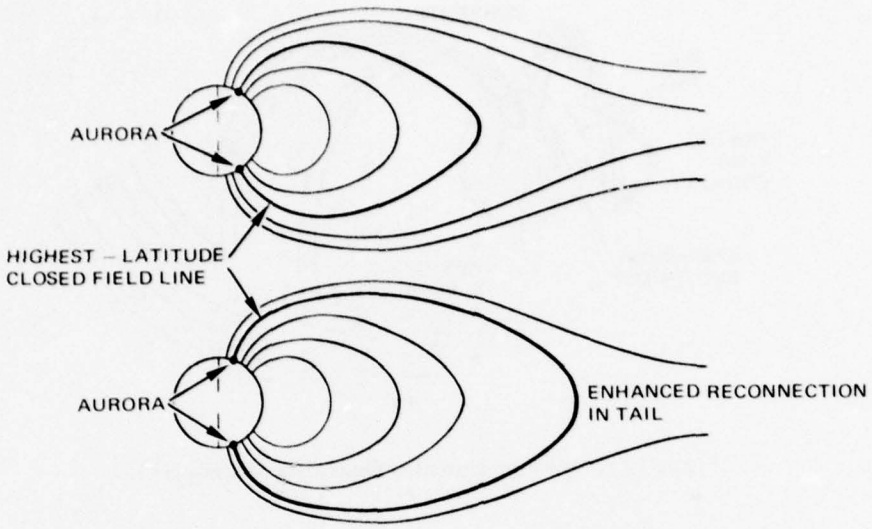

Figure 11. Poleward motion of the aurora due to enhanced reconnection in the magnetotail.

circuit, along with the field-aligned (or Birkeland) currents. The following models of Akasofu (and others) use current systems consisting of day/evening asymmetric ring current, field-aligned currents into the dawn/dusk oval, and the auroral electrojet (fig 12). The low-latitude magnetic field measurements require an eastern (dusk/dawn) tail current (opposing the normal dawn/dusk current). Akasofu recognized that the loss of westward current is equivalent to the needed eastward current, and so he allowed the tail current to be shunted into polar current (fig 12A). Since this recognition, people have worked on more sophisticated 3D models (fig 12B) (Fukushima, 1972; Yasuhara and others)* that include the partial ring current.

Akasofu, in his early work (1970), also developed a concept of the simple time variations of the current system during a substorm. Notice from figure 13 that the region of reduced plasma density spreads radially outward along the neutral sheet. The spreading down the tail causes the poleward motion of the aurora, explained earlier, while the cross-tail spreading causes the endpoints of the field-aligned magnetospheric currents to move westward, creating a westward surge of auroral activity.

AREAS OF CONFLICT: AKASOFU AND THE DYNAMIC AURORAL OVAL

Akasofu first pointed out in 1973 that the oval's position varies with the direction of the interplanetary field, thus affecting auroral electrojet (AE) measurements.

---

*Fukushima, N, "Polar magnetic substorms," Planet Space Sci, 20, 1443, 1972

Yasuhara, F, Kamide, Y, and Akasofu, SI, "A model of the magnetospheric substorm," Planet Space Sci, 23, 595, 1975

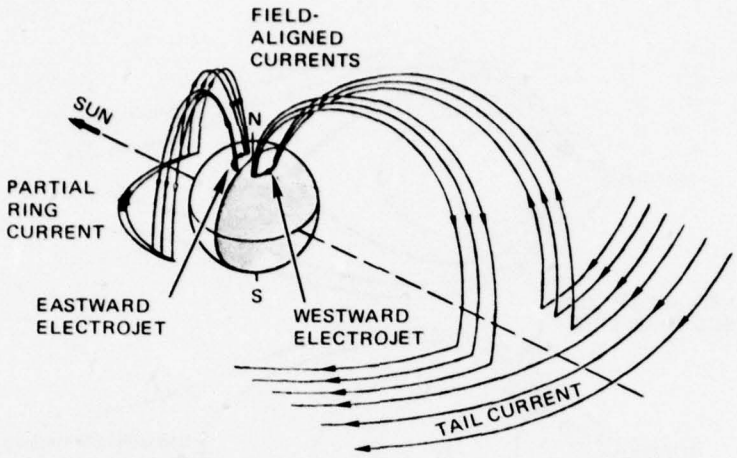

Figure 12A. Substorm current systems after Akasofu (1972).

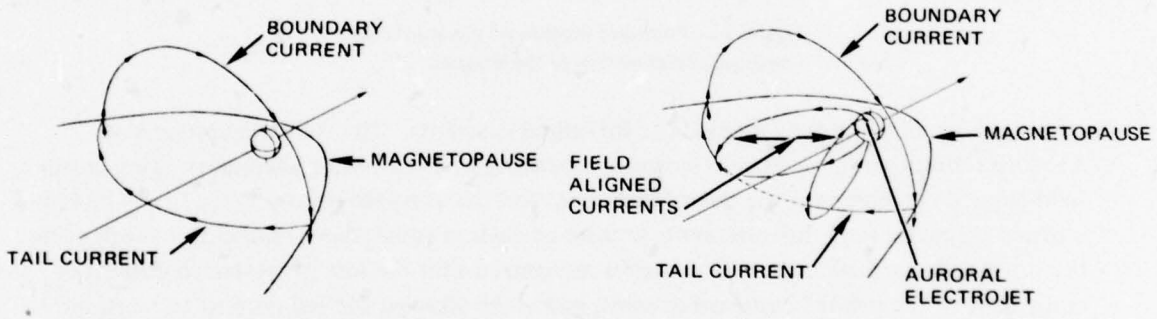

Figure 12B. Substorm current systems after Fukushima (1972).

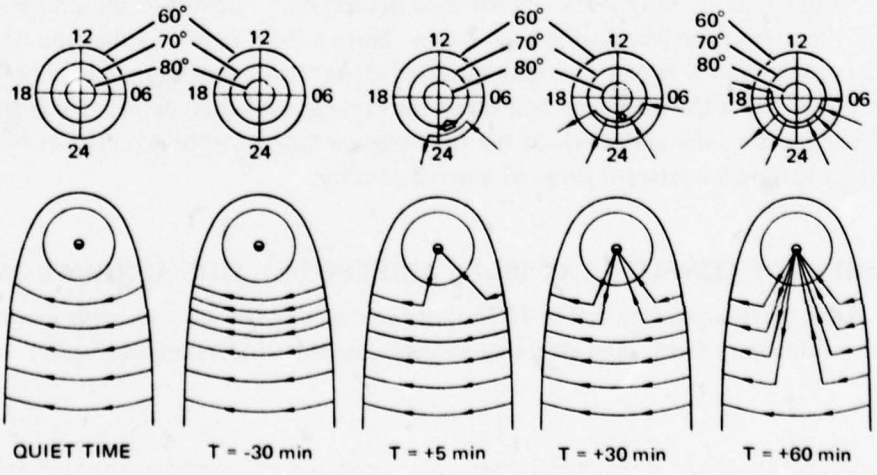

Figure 13. Development of a magnetospheric substorm, as the crosstail current is deflected to the polar region.

In a process exactly like that indicated in the early development of substorms (McPherron, 1972*), the enhanced merging at the magnetospheric nose due to the southward turning of the IMF moves the polar cusp equatorward and causes an expansion of the open polar cap (auroral oval) (see fig 6, 11).

Akasofu contends that variations in this near-reversible process are continually present, and are the cause of many of the conflicts that will be mentioned later. Specifically, motions of the oval (and its always-present but slight electrojet) will cause ground-level magnetic variations that may mask or obscure the actual substorm onset as observed by ground-level magnetometers. More important, however, is the fact that when the IMF has a large northward component, the nose merging decreases to near zero, and the auroral oval contracts far poleward (up to $\sim 80^\circ$). If the oval is above $\sim 70^\circ$ dipole latitude, the magnetic activities associated with substorms will not be seen.

Therefore, as Akasofu has been strongly pointing out, studies that use the auroral electrojet indices (or magnetic signatures at nominal auroral stations) will not see activity when IMF B_z is northward, and so all "activity" will be strongly correlated to southward IMF.

THE GROWTH STAGE: AKASOFU VS McPHERRON

The basic phenomenology of the magnetospheric changes following a southward turning of the IMF (given by McPherron (1972), fig 8) is accepted by Akasofu. It is McPherron's interpretation of succeeding events that Akasofu takes exception to. McPherron envisions that towards the end of the "growth stage," the plasma sheet at $\sim 10R_E$ becomes thinner (narrower) because of increasing tail magnetic pressures caused by a southward IMF. He suggests that this thinning creates a neutral point field reconnection, marking the onset of the expansive stage of the substorm. In this theory, the tail is the location of the triggering instability.

Akasofu, on the other hand, believes that an anomalous resistivity in the field-aligned current flow causes enhanced current flows along the field lines into the auroral oval. This earthward flow disrupts the crosstail currents because there is no plasma to carry it. This disruption happens at the same tail location at which McPherron's model displayed the initial thinning (ie, $10R_E$). The tail plasma sheet thins, creating a reconnection point, and the substorm expansion phase begins.

The argument goes deeper, however. As Akasofu stresses, there is ample evidence that substorms are as common with the IMF northward as they are with it southward, albeit the substorm energy expenditures are way down. Remember that McPherron's model used the enhanced merging from the IMF being directed southward to trigger the substorm mechanism. Unfortunately, McPherron deals with Akasofu's "northward" events by ignoring them on the grounds that the total energy release therein is small and, therefore, "they don't represent any great change within the magnetosphere." Akasofu's point was missed entirely – how do these "northward" substorms trigger? Certainly enhanced tail pressures cannot be

*McPherron, RL, "Substorm related changes in the geomagnetic tail: the growth phase," Planet Space Sci, 20, 1521, 1972

the source, and then McPherron must postulate that the substorms with the IMF directed northward are intrinsically different from the substorms with the IMF southward, contrary to any evidence available today.

CONCLUSIONS

The basic mechanism of magnetospheric energy release through substorms is becoming understood with the aid of satellite measurements. The energy dissipation is in the auroral E-region, and comes about through particle precipitation and current (joule) heating. This energy input into the polar ionosphere and neutral atmosphere is the cause of the *ionospheric substorm* portion of Akasofu's substorm manifestations, and the ensuing global ionospheric disruptions impact upon communication systems using ionospheric propagation. Therefore, understanding the temporal and spatial substorm variations should aid in determining the temporal and spatial variations in the global ionosphere. Extending the present DMSP satellite capabilities to monitor real-time auroral activity would provide energy concentration inputs for ionospheric storm models. Ionospheric storm modeling, which is in its early stages of development, is discussed in chapter 2.

CHAPTER 2: IONOSPHERIC STORMS

INTRODUCTION

Ionospheric storms are the F_2-region variations (including enhancements and depletions in electron density, as well as raising and lowering of the F_2 peak height) associated with magnetic storm variations. The consensus in the field is that these storm-time ionospheric changes are of secondary nature caused by the geomagnetic storm aftereffects. The resultant changes are an outcome of several competing *and* cooperating processes and, therefore, each individual storm pattern appears complex and unpredictable. Several workers have developed "average" storm patterns for given locations as well as general global-type average morphologies. Unfortunately, the individual storms do not, in general, follow these average events, making the "average" storm effectively useless for practical propagation predictions.

The major problems in studying ionospheric storms stem from the total number of variables that can affect the electron density changes. These include (1) the time of the sudden commencement – if the storm starts during the high-electron-density day, the effects could be different than at night; (2) the state of the neutral thermosphere – this controls the whole chemical loss process and may affect the propagation of the disturbance equatorward; (3) the actual magnetic field and electrical current variations – these are the driving force behind the ionospheric disturbance; (4) the position (on the earth) of the recording station relative to the magnetic and electric current changes – a short-time scale variation will cause very localized effects (Park, 1974).* It is likely the neglect of one (or more) of the above factors in every analysis has led to the apparent inability to understand ionospheric storm behavior.

Ionospheric storms are observed with two basic experimental probes: (1) hf vertical incidence sounders yielding basically the density and altitude of the F-region peak; and (2) total electron content (TEC) systems which use the Faraday rotation of vhf satellite signals to give the integrated electron density along the signal path. The measurements are complementary because the TEC system is also affected by the electron density above the F-region peak, a region which the vertical incidence sounder can obviously not probe.

This report reviews a large set of the F-region ionospheric storm analyses, the ionospheric processes believed to be involved, and the "state of the art" in storm prediction. A final section investigates the usefulness of this state of the art to real-time propagation prediction and hf frequency management. It also suggests future study to enable the definition of storm morphology.

---

*Park, CG, "A morphological study of substorm-associated disturbances in the ionosphere," J Geophys Rev, 79, 2821, 1974

FEATURES OF THE IONOSPHERIC STORM

AVERAGE STORM EFFECTS

Because of the large storm-to-storm variations, many workers have developed "average storm patterns" in attempts to describe and understand ionospheric storm behavior. Mendillo (1971)* (using TEC measurements) observed that there are two distinct time patterns superposed on these storms: (1) storm-time variations (D_{ST}) reckoned from time of sudden commencement; (2) local time variations (SD) reckoned by local time with the sudden commencement in day 1. The (D_{ST}) (storm time) variations have a distinct pattern (fig 14A), with a 12-hour positive phase followed by a 72-hour negative phase. The (SD) (local time) pattern (fig 14B) indicates that this large positive effect is at the sunset period on the first day of the storm. Again, notice that any given storm may not follow this average behavior. In particular, the positive phase appears to be dependent on the time of the sudden commencement, and many storms (usually with local nighttime sudden commencements) have no positive phase. On the other hand, work done at NOSC indicates that during the winter season the whole storm-time effect may be a positive phase.

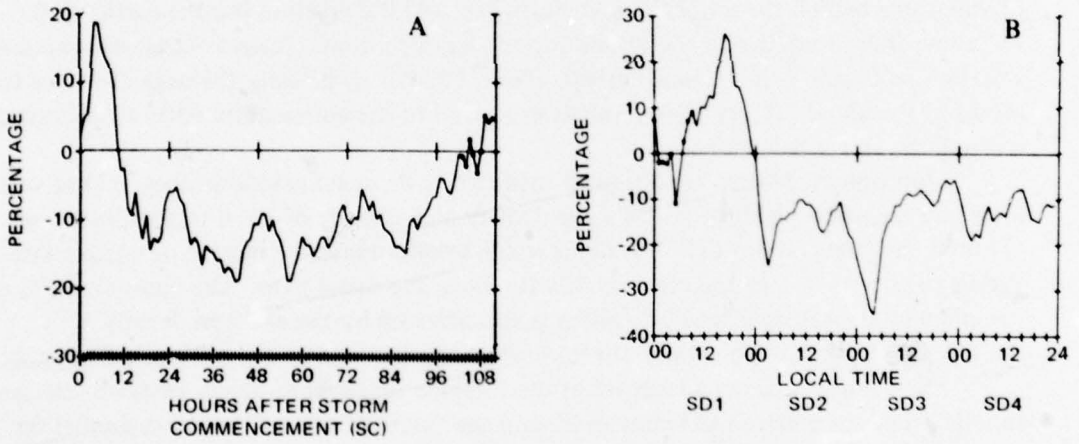

Figure 14. TEC "average storm" variations showing both storm time (D_{ST}) and local time (SD) dependence (Mendillo, M, "Ionospheric total electron content behavior during geomagnetic storms, Nature, 234, 23, 1971)

Mendillo states that this analysis was used to look for seasonal variations in storm behavior, and that no great seasonal differences were discovered. This is somewhat surprising because the above-mentioned analysis at NOSC indicates very strong seasonal differences in storm variations.

*Mendillo, M, "Ionospheric total electron content behavior during geomagnetic storms," Nature, 234, 23, 1971

NEGATIVE PHASE

The "average storm-time variation" is found to be an increase in electron density (positive phase) followed by a decrease (negative phase). In this section the negative (or main) phase and the physical mechanisms are discussed.

The negative phase of the ionospheric storm appears to be caused by the neutral upper atmosphere's reaction to the energy deposition of geomagnetic storms. This energy is deposited in the upper atmosphere in two forms – particle dumping and the resistive "joule" heating of electrical currents. The particles are mainly dumped near the geomagnetic "cusp" region, although there is a spread around the auroral zone as well as down to mid-latitudes. Recently it has been determined that the electrical currents in the auroral zone can be very large and hence cause significant joule heating. These energy inputs modify the high-altitude global wind systems and also cause gravity wave trains to propagate outward (equatorward and poleward) with the apparent effect being a turbulent mixing of the neutral atmosphere. This mixing is followed by an increase in the chemical loss rates which should result in a net decrease in electron density as well as an altitude increase in the peak height.

Other explanations for the electron density decrease invoke neutral wind or electric field transport mechanisms. The transport to the higher-loss region necessitates a downward motion of the F-layer, and this is contradictory to experimental evidence. Therefore, it is usually assumed that the loss rates themselves are changed during the negative phase of the storm, with the change mechanism being the neutral thermosphere. This manner of change explains both the decrease in electron density and the increase in the altitude of the F-region peak.

POSITIVE PHASE

There is general agreement that the positive early storm effects are caused by transport of the positive ions and electrons. Vertical transport into lower-chemical-loss-rate regions (ie, higher altitudes) by either thermospheric winds or electrodynamic forces is likely to dominate any horizontal transport mechanism because of scale height effects.

Prolss and Najita (1975)* suggest that the electrodynamic uplifting is responsible because evidence (both experimental and theoretical) is that the wind motions would be zonal (east-west) component dominated (causing no upward transport along field lines). Lanzerotti and others (1975)** showed that the large local evening enhancements in some storms are associated with positive bay geomagnetic disturbances, which indicate the existence of large electric currents that would create upward electrodynamic forces. Mendillo (private communication) has observed this association also, but finds no relationship of the electron density enhancement magnitude to that of the positive bay. Papiagannis, Mendillo, and Klobuchar (1971)*** found that the maximum total electron content (TEC) during

---

*Prolss, GW, and Najita, K, "Magnetic storm associated changes in electron content at low latitudes," J Atmos Terr Phys, 37, 635, 1975

**Lanzerotti, LJ, Cogger, LL, and Mendillo, M, "Latitude dependence of ionospheric total electron content: Observations during sudden commencement storms," J Geophys Res, 80, 1287, 1975

***Papagiannis, MD, Mendillo, M, and Klobuchar, JA, "Simultaneous storm-time increases of the ionospheric total electron content and the geomagnetic field in the dusk sector," Planet Space Sci, 19, 503, 1971

these positive phase periods averaged much higher than usual local noontime value, with the positive phase being a sunset period phenomenon.

LARGE AND RAPID DROPS IN TEC NEAR SUNSET PERIOD

In examining the TEC data of AFCRL's Sagamore Hill Radio Observatory at Hamilton, Mendillo and others (1974)* observed that on a few occasions an abnormally large and rapid drop in TEC is observed near the sunset period. They find the decay rates (dN_T/dt) to be more than 10 times greater than the respective monthly mean. Because they did not believe that any change in the loss process could be of such drastic nature, their conclusion was that due to plasmaspheric contraction the radio propagation path was crossed by the midlatitude trough. Mendillo and others developed a strong case for the equatorward movement of the plasmapause boundary causing the sharp decreases. The Hamilton TEC subionospheric point L value is 2.8, and movements of the boundary into this region are not impossible. However, data from the 8 March 1970 event indicate that the sudden decreases exist down to Arecibo, with an L value of 1.4 (fig 15). This is far equatorward of any reasonable plasmapause boundary, and so the Mendillo explanation would seem unreasonable.

Davies (1974)** developed an explanation for the sudden decrease, in which he allows a sudden atmospheric mixing to cataclysmically increase the loss rates. The sudden mixing is caused by a "shock front" (see appendix) of turbulence propagating equatorwards from a "supersonic" disturbance in the auroral zone. For simplicity, Davies considers the disturbance to be particles dumped out of the magnetosphere into the geomagnetic cleft (cusp), which is at approximately the local noon longitude. For propagation velocities of 4°-5°/h (~150 m/s), the front will propagate equatorwards in such a manner as to cause the sudden depletions with the time lags derived for the 8 March 1970 event (see appendix).

REVIEW OF PAST WORK IN IONOSPHERIC STORMS

SOME OBSERVATIONS AND ATTEMPTS AT GLOBAL MORPHOLOGY

Many workers in the past have examined data from one or more stations and developed storm morphologies. One of the first was a study done by Matsushita (1959)***, who found that the equator region had positive storm effects while mid and high latitudes

---

*Mendillo, M, and Klobuchar, J, An Atlas of the midlatitude F-region response to geomagnetic storms, AFCRL Technical Report 74-0065, February 1974

**Davies, K, "Studies of ionospheric storms using a simple model," J Geophys Res, 79, 605, 1974

***Matsushita, S, "A study of the morphology of ionospheric storms," J Geophys Res, 64, 305, 1959

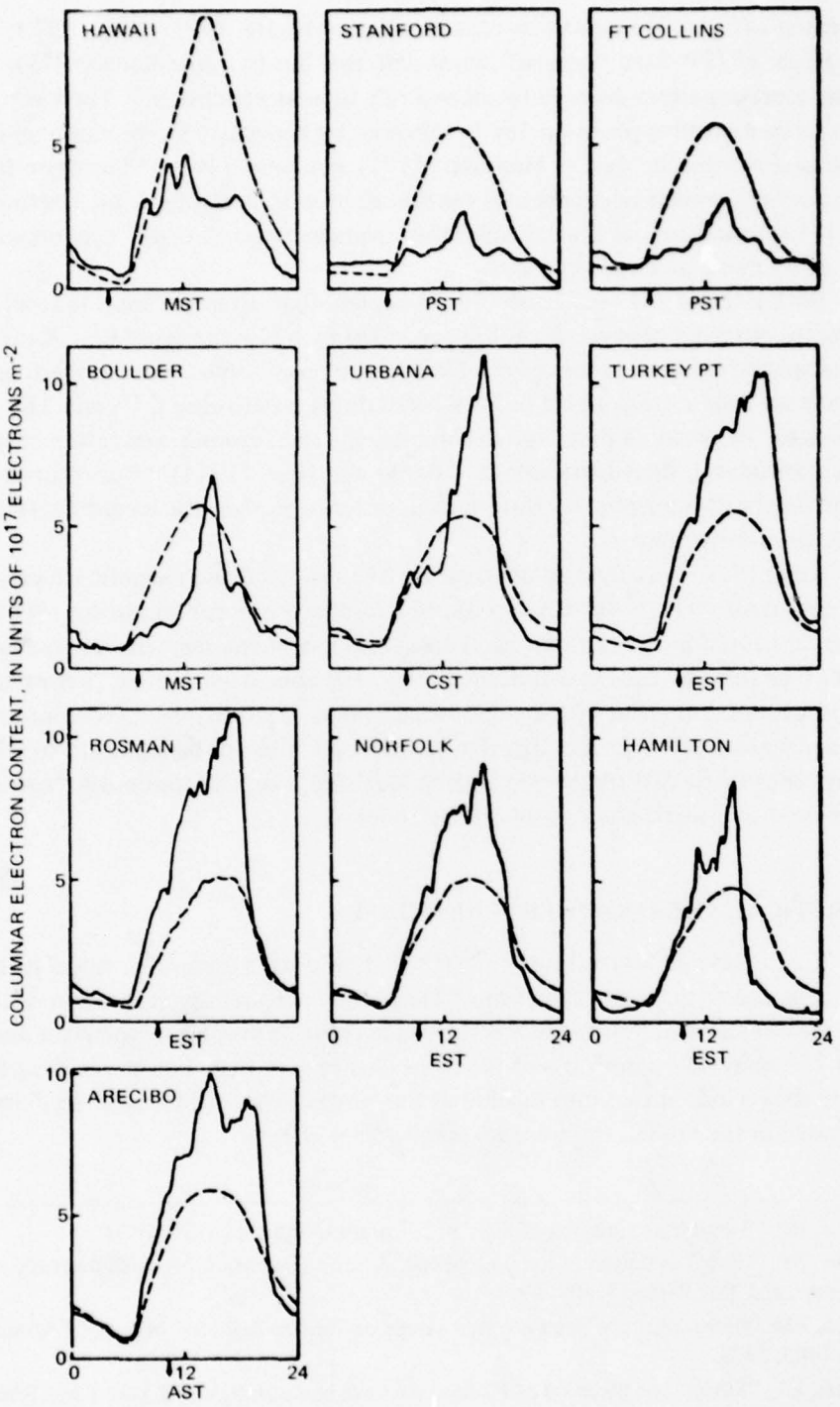

Figure 15. TEC variations for ionospheric storm of 8 March 1970 for several stations. The dotted lines indicate the average diurnal patterns for each station. (Klobuchar, JA, and others, "Ionospheric storm of March 8, 1970," J Geophys Res, 76, 6202, 1971)

had negative effects. More recent works (Prolss and Najita, 1975; Kane, 1973; Kane, 1975; Rush, 1972)* have "typical" storm patterns, but to quote Kane (1973), "deviations from the average pattern seem to be more a rule than an exception." The basic pattern appears to be a positive phase on day 1, followed by a negative storm phase on day 2, recovering somewhat on day 3. Mendillo (1971) and Jones (1971)** indicate that if the sudden commencement occurs before sunrise, there will probably be no positive phase. Kane (1973) found that at low latitudes the "average pattern" of f_0F_2 increases is rarely seen — often there are large decreases.

Both Kane (1973) and Rush (1972) explain that often different ionospheric behavior patterns are observed between locations separated by a few thousand km. Kane postulates that ionospheric storms are the result of local "typhoon" type events in the thermosphere, and hence we need a *close* global network of stations monitoring f_0F_2 and TEC. These disturbances "originate in polar and auroral regions and forming convection cells, descend to lower latitudes in turbulent fashion." Banks and Nagy (1974)*** also forward this cyclonic theory of ionospheric disruptions in order to explain the localized effects some ionospheric storms cause.

Park (1974) described an observation of an isolated geomagnetic substorm of moderate intensity (K_p = 40) that produced a *localized* ionospheric storm over the eastern continental United States. In that local area this ionospheric disturbance was similar to the behavior seen during major ionospheric storms. His conclusion is that "ionospheric storms can be understood in terms of the superposed effects of substorms." The impact of this is that the planetary geomagnetic disturbance indices would not be expected to relate strongly to many ionospheric disturbances in a given localized area, and that more "zonal" parameters must be used to understand ionospheric behavior.

THEORETICAL THERMOSPHERIC RESPONSE

Richmond and Matsushita (1975)**** developed a computer model of the thermospheric response to magnetic substorms. They conclude that the generation of large-scale gravity waves causes an impulse-like disturbance front to propagate poleward and equatorward at 750 m/s. The amplitude of the front decays very little before reaching the equator. Also, ion drag winds are set into motion at the auroral oval, but because no diurnal variations are included in the model, there are no longitudinal effects.

---

*Kane, RP, "Storm time variation of F2 region," Annls Geophys, 29, 25, 1973

Kane, RP, "Global evolution of the ionospheric electron content during some magnetic storms," J Atmos and Terr Phys, 37, 601, 1975

Rush, CM, "Some effects of neutral wind changes on the low latitude F-region," J Atmos Terr Phys, 34, 1403, 1972

**Jones, KL, "Storm time variation of F2-layer electron concentration," J Atmos and Terr Phys, 33, 379, 1971

***Banks, PM, and Nagy, AF, "Cyclonic disturbances and their consequences in the thermosphere," Geophys Res Letters, 1, 305, 1975

****Richmond, AD, and Matsushita, S, "Thermospheric response to a magnetic substorm," J Geophys Res, 80, 2839, 1975

Notice that the 750-m/s disturbance propagation velocity is considerably higher than the 150 m/s inferred from data. It may be that the calculated winds following the disturbance with velocities of 200 m/s are the mixing source.

RESULTS OF PRESENT WORK

We have taken vertical incidence sounder data from Vandenberg, California, and Honolulu, Hawaii, for several ionospheric disturbances between May 1973 and the present. Using a pre-event average defined by the 5 days prior to the sudden commencement, we calculated the average variations of the storms as Mendillo did. We found a distinct seasonal difference that was separated as summer (May-Aug) and winter (Nov-Feb) (fig 16A, B).

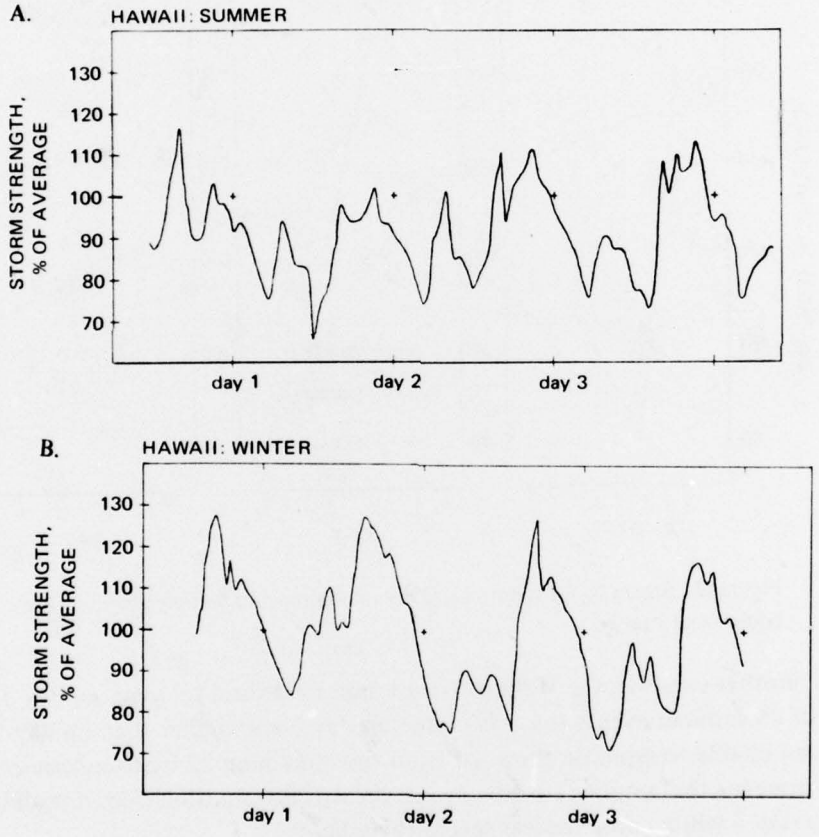

Figure 16A, B. Average f_0F_2 storm variations (using local time) for Hawaii, summer and winter storms.

The Hawaii station quiet average day had a very peaky density function (around noon) for most events. This fact made the Honolulu data rather intractable because slight shifts (along the time axis) of the storm data would cause large enhancements and depletions even if the daily maximums did not vary. These variations, when averaged, almost cancel out and yet leave large standard deviations in the error analysis. Basically, the problem is that the

ionospheric storm modified the diurnal variations in a presently unpredictable manner. In an attempt to find some predictable facet of a storm, we next took the daily peak (ignoring time information) and developed an average storm behavior for Hamilton (Wallops Island AFCRL data), Vandenberg, and Hawaii (fig 17A, B, C). Again, a strong seasonal dependence is noted. Notice that Wallops Island summer shows a large increase on day 1, followed by a strong decrease on day 2, with a recovery phase on days 3 and 4. Examining the second day of the storm, one discovers that four of the 24 summer events studied in Wallops Island data actually show increases above normal "quiet day."

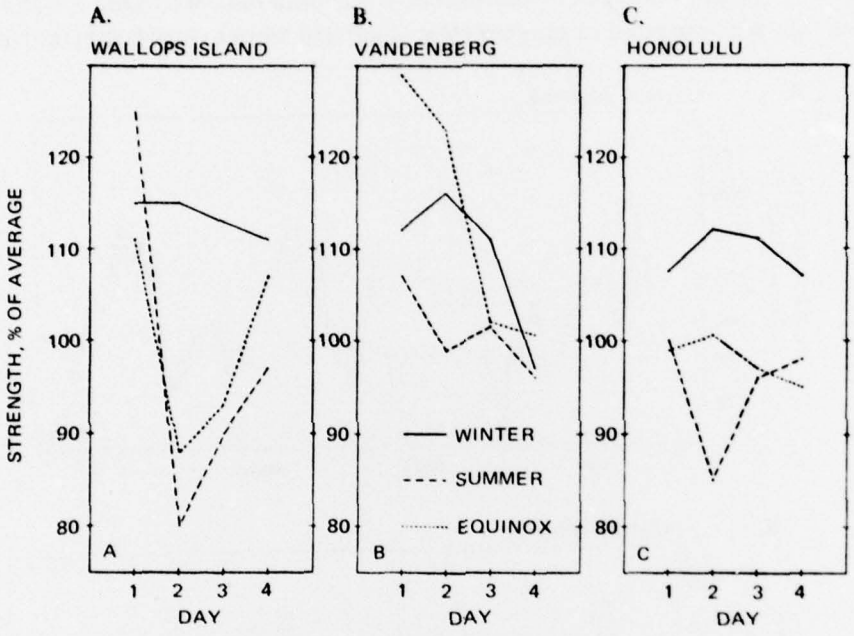

Figure 17. Storm F_0F_2 variations (daily maximum) for summer, winter, and equinoctial storms.

As another exercise, the Wallops Island data were used to compare day 3 to day 2. In 14 out of 26 summer events the f_0F_2 value on day 3 was higher than on day 2; so far we have been unable to separate those 14 from the remaining 12 by using *any* other parameter. This means that on day 2 of the event, present information does not allow prediction on whether day 3 will be more or less severe than day 2.

The above indicates that although an "average" storm may be defined, we cannot accurately estimate the ionosphere variations for a given event by using the presently available information. Although a storm *generally* shows decreases in the F-region electron density, neither the amount of this decrease nor its temporal variation appears related to the magnetic storm variations as described by Ap values.

EVALUATION OF AN OPERATIONAL MODEL

Patton and Cohen (1971)* have developed a prediction model in order to allow the USAF to use real-time frequency management on certain hf systems (OTH radar). These authors decided to deal with only negative storm phases (and predictions), which have the largest system impact because they cause hf system outages. The model was developed to fit the storm morphology described in Obayashi (1964) and Davies (1965) (Davies tabulated Matsushita's (1959) data on average behavior).** Davies states of his table: "the overall average is therefore not representative of a single storm in either of those seasons (summer, winter)." The data indicate an approximate 15% decrease at the equator varying to ~40% decrease at 60° latitude.

The model incorporates seasonal and latitudinal variations by means of a "local K index" K_L which is averaged with the Kp: $K = (1.5Kp + K_L)/2.5$. K_L has a maximum at summer high latitude and a minimum at winter low latitude in the form:

	summer	winter
0°	$K_L = 3$	$K_L = 2$
90°	$K_L = 9$	$K_L = 7$

The storm MUF is then described by:

$$\frac{\text{MUF storm}}{\text{MUF quiet}} = \frac{13.1 - K}{11.1}$$

This model predicts average ionospheric storm responses according to Obayashi and Matsushita morphologies. As described in the last section, the data studied at NOSC indicate that lower-latitude regions (Hawaii) may be considerably more responsive than midlatitude regions. Also, in 18 winter events measured at Wallops Island, Virginia, only one decreased to significantly below average. In other words, the above-described model does not match the ionospheric storm responses accumulated at NOSC.

FUTURE CONSIDERATIONS

It has been emphasized that the presently available data set is not spatially dense enough to develop an understanding of ionospheric storms. The future should thus initially include the operation of such a measurement network covering at least the Pacific area so that complete storm morphologies can be developed. Once this assessment process is completed, *then* perhaps a prediction capability will be at hand. A stop gap measure being undertaken by Bleiweiss and Argo (private communication) is the using of the AWS sounder network surrounding the Pacific in a real-time ionospheric assessment program. We now know that the wide separation of the sounders will probably allow only very degraded analysis, and so further effort *must* be expended.

---

*Patton, DE, and Cohen, ML, "A simple magnetic storm prediction model suitable for real-time frequency management," Raytheon report published at ARPAOHD Tech Review, 17-18 March 1971

**Obayashi, T, Research in Geophys, chapter 14, vol 1, MIT Press, Cambridge, 1964

Davies, K, Ionospheric Radio Waves, Blaisdale Publishing Co, Walthrow, MA, 1965

In short, the ionospheric storm can be viewed as a meteorological process (albeit thermospheric) with the attendant prediction problems. A close network of sounders will allow the measurement of "frontal" motion and the movement of "high" and "low" density regions. But until these highs and lows can be viewed as finite, moving regions, their effects on a single ionospheric measuring system *must* appear capricious.

APPENDIX:
GEOMAGNETIC STORM EFFECTS ON THE MIDLATITUDE IONOSPHERE: A "SHOCK FRONT" TURBULENT MIXING MODEL AND CALCULATIONS OF THE FRONT SHAPE

INTRODUCTION

Ionospheric storms are commonly caused by geomagnetic activity, often in the form of geomagnetic storms. Ionospheric storm behavior is highly variable, because of the several sources of enhancements and depletions. General morphological studies have been done although individual events may be far from the norm.

Generally, at midlatitudes the F_2-layer peak density undergoes an initial enhancement (positive phase), followed by a sharp drop to below the "quiet" average density. The following several days and nights may remain enhanced or depleted. The positive phase may be explained by electrodynamic lifting (the theory of equatorward winds blowing the ions up the field lines has lost favor) of the ions into lower-loss regions, causing density increases. The negative phase may be either a pushing down of the ions into higher-loss-rate regions; or, as will be suggested here, the propagating of turbulent waves out of the polar region toward the equator, causing increased mixing of the neutral atmosphere, which in turn will yield an increased loss rate at all altitudes.

Davies (1974) suggested that there is a heat source on the auroral oval which has an apparent localized motion that is greater than the propagating velocity of the disturbance. This gives rise to a wake, or "shock front," that propagates equatorward and results in a change in the chemical concentration at F-layer heights. The neutral concentrations will return slowly to undisturbed conditions over a period > 24 hours, which constitutes the "negative phase" of an ionospheric storm.

In this paper we shall show calculations of the shock front shape for various conditions – an outcome of this model is that a localized source area (on the oval) is responsible for the portion of the shock front at an observer's location. In other words, an energetic event along southern Greenland may affect the Eastern United States, leaving the remaining portion of the world unchanged. These localized storms are very real (Park, 1974), and, using this present theory, we may learn to forecast them.

THE MODEL

The Davies model considers a point heat source located on the auroral oval (on the noontime magnetospheric cusp) that moves with the rotation of the earth. The disturbance, here presumed to be gravity waves, propagates radially outward at a velocity of 2°–5° per hour. Nighttime joule heating would have similar effects, although it would be an extended source.

The Feldstein oval is placed at 78° (noon) during quiet conditions, and Davies uses a 2°-latitude change equatorward per unit change in the planetary magnetic index K_p. Hence, the source point is at a latitude ϕ_s:

$$\phi_s = 78° - 2\,K_p \quad .$$

Considering only the propagation towards lower latitudes, the storm front will appear as a "wake" similar to that made by a speedboat. As it moves through an atmospheric region (at the E-layer input altitude), a cataclysmic turbulent mixing takes place, which may move the turbulent-mixing boundary (usually at an altitude of 100–120 km) to heights > 200 km. Numerical models of the ionosphere (Ruster and Dudeney, 1975) indicate that height increases in this boundary level result in large decreases in F-region electron density, caused by changes in the O/N_2 ratio. Because of the "shock front" moving through, these changes can occur rapidly. The return to normal quiet conditions will be at the slow rate suggested by Rishbeth and Hanson (1974).* See figure A1.

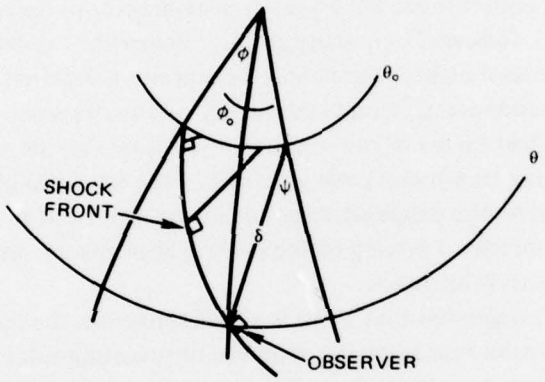

Figure A1. Geometry of the shock front propagation calculation.

θ_o is the source latitude, θ is the observer latitude, ψ is the angle of propagation from the normal.

ϕ is the angle swept out by the source in the time the disturbance propagates a distance δ, so ϕ–ϕ_o is the longitude difference of source and observation point. Notice that it is latitude dependent.

The propagation path length δ is described by

$$\delta = a \cdot \phi_o ,$$

where $a = d\delta/d\phi = \cos \psi$, hence ψ is constant; notice $a = v/15$, where v is the propagation velocity (in deg/h)

Using spherical trigonometry,

$$\cos \theta = \cos \theta_o \cos \delta - \sin \theta_o \sin \delta \cos (\phi_o - \phi)$$

and

*Rishbeth, H, and Hanson, WB, "A comment on plasma 'pileup' in the F-region," J Atmos and Terr Phys, 36, 703, 1974

$$\phi_o - \phi = 2 \tan^{-1} \left\{ \frac{\sin (s-\theta) \sin (s-\theta_o)}{\sin (s-\delta) \sin (s)} \right\}^{1/2}$$

where $s = (\theta + \theta_o + \delta)/2$.

Since we are interested in the longitude $(\phi_o - \phi)$ that affects a given latitude with a source at (ϕ_o, θ_o), we are given θ, θ_o, a, $\cos \psi = \sqrt{1-a^2}$. Using the spherical trigonometry law of cosines

$$\cos \theta = \cos \theta_o \sqrt{1 - \sin^2 \delta} - \sin \theta_o \sin \delta \cos \psi$$

or

$$\cos \theta + \sin \theta_o \sin \delta \cos \psi = \cos \theta_o \sqrt{1 - \sin^2} \quad .$$

Squaring and regrouping:

$$\sin^2 \delta \left[\cos^2 \theta_o + \sin^2 \theta_o \cos^2 \psi \right] +$$

$$\sin \delta \left[2 \cos \theta \sin \theta_o \cos \psi \right] +$$

$$\cos^2 \theta - \cos^2 \theta_o = A \sin^2 \delta + B \sin \delta + C = 0 \quad .$$

Solving for $\sin^2 \delta$ and using the Law of Sines ($\sin \delta / \sin (\phi_o - \phi) = \sin \theta / \cos \psi$), we get

$$\sin (\phi_o - \phi) = \frac{\sin \delta}{\sin \theta} \sqrt{1-a^2}$$

with

$$\sin \delta = - \frac{B + \sqrt{B^2 - 4 AC}}{2A} \quad .$$

The two roots indicate the fact that there is poleward propagation as well as equatorward, so we choose the positive root, as we are interested in midlatitudes. The negative root corresponds to over-the-pole propagation to midlatitude.

By evaluating δ, and $\phi_o - \phi$ as a function of latitude, one obtains the shock front curve, and also the path along which the shock front "appears" to propagate from the source equatorward. Figure A2 shows the fronts and paths for the propagation velocities 2°, 3°, 4°, 5°/h. The spiral structure of the fronts is evident, but notice that an energy input for a short period will cause only a portion of this spiral to develop (fig A3). That portion will propagate equatorward along the propagation paths, so by setting the current velocity path on the observer's location, one can determine the high-latitude region of importance. Greenland will

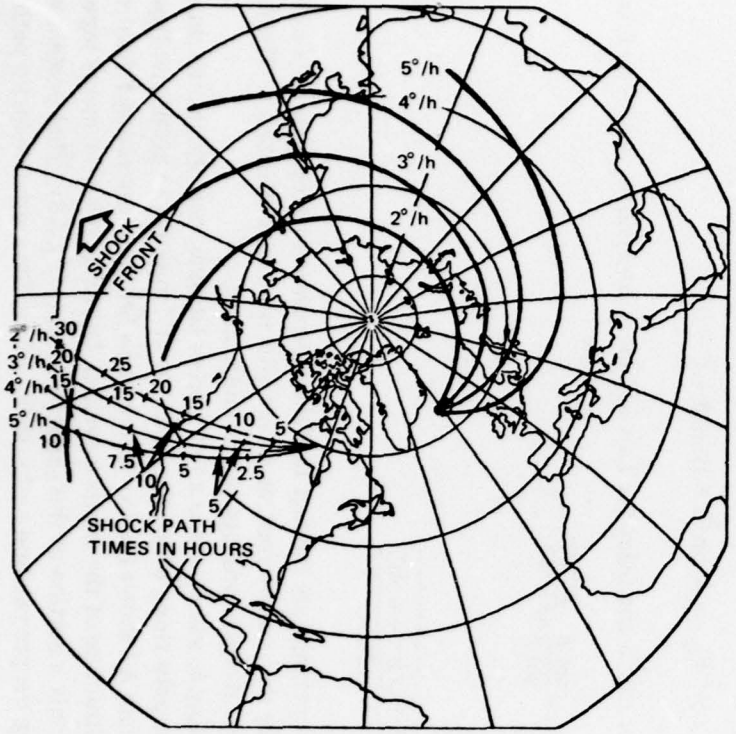

Figure A2. Shock path and shock fronts for several propagation velocities.

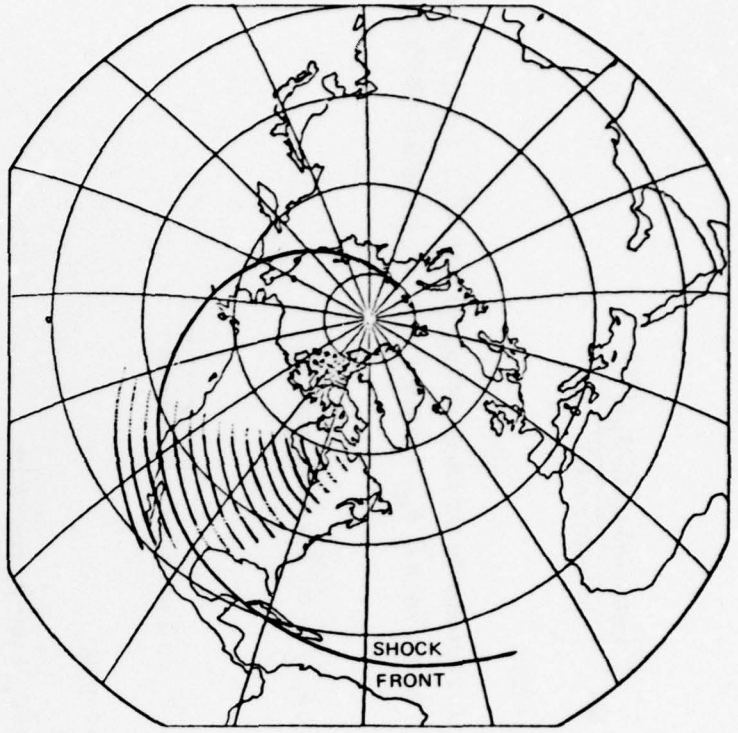

Figure A3. Diagram showing how only a portion of the shock front may develop and propagate, creating localized disturbances.

affect the Atlantic seacoast, while the western Great Lakes develop shock fronts that sweep across the California-Hawaii Pacific area.

DISCUSSION

The outcome of this model (the Davies model) is that a mixing front should propagate equatorward from the auroral zone, with a rapid depletion of the F-region (caused by greatly enhanced loss rates) being observed. The mixing effectively raises the turbopause, or lowers the boundary of diffusive equilibrium, which increases the molecular nitrogen concentration relative to atomic oxygen; this increases the effective loss rate at F_2 peak altitudes, followed by a decrease in the peak electron density. Therefore, if the model is valid, a latitude dependence in the "sudden depletion" time should be observed, and should fit the predicted times of arrival.

Perhaps more important is the conclusion that a specified longitude along the auroral oval is responsible for the portion of the front passing over any other latitude, longitude position, and that energy deposited in this region is expected to affect only a localized path (fig A3).

The 8 March 1970 ionospheric storm has had a complete data compilation from US stations measuring the ionospheric total electron content (TEC) (Klobuchar and others, 1971*), which roughly relates to F_2 peak electron density. One set of the observing stations lies along a line corresponding to our postulated "propagation path," and so the propagation time can be checked and calculated. Another set of the stations lies approximately along a constant geomagnetic latitude line, so an estimate of the longitude extent of the front can be made. Figure A4 shows the deviations from the mean of the electron content for the storm day for both latitude and longitude ordering. Notice that along the propagation path the stations do show increasing delays with decreasing latitude. Figure A5 compares these onset times with model predictions (for various propagating velocities), with a velocity $\sim 3\frac{1}{2}^\circ$/h fitting the data closest. The longitude chain does indicate a strong dependence on longitude, with the eastern stations having large depletions at the predicted time, and towards the west there are progressively smaller effects, until Hawaii has no discernible decrease. This is expected because the Eastern section was in late morning conditions, while Hawaii and Stanford were presunrise; if the energy is dumped in the noontime cusp for a short period, the effects should not extend into the sunrise longitudes.

For this single event (the most thoroughly documented) the model provides an excellent description; that it will work this well in all cases is unlikely, but more extensive testing is necessary. A major problem exists in studying ionospheric storms. There are many competing *and* cooperating processes that act in varying magnitudes to make each event individual. Unfortunately these very differences impede any statistical evaluation of ionospheric storms in general. For example, if the "positive phase" is extraordinarily large, the depleting effects of one front (as well as downward motion) may leave a net increase in the F_2 peak, and so, according to some researchers, no negative phase occurred. The model described here predicts sudden depletions in the F-region, with no regard to the initial or final value of F-region density. Any other approach would be misleading.

---

*Klobuchar, JA, and others, "Ionospheric storm of March 8, 1970," J Geophys Res, 76, 6202, 1971

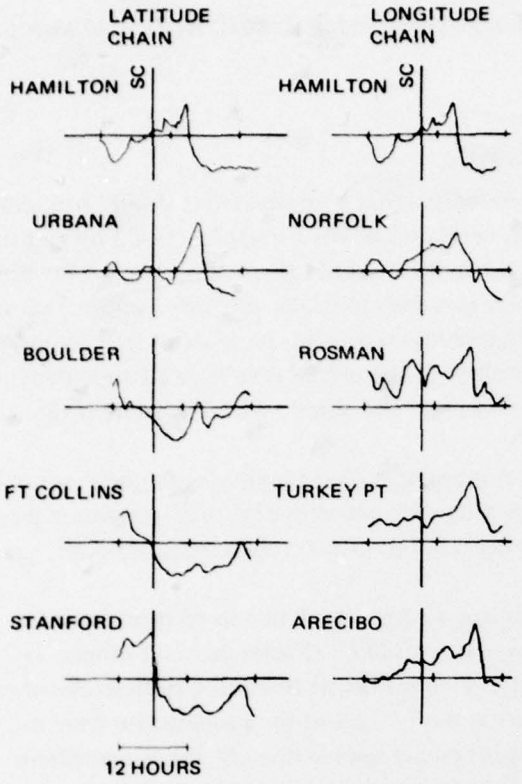

Figure A4. Deviations of TEC from mean for the 8 March 1970 event showing both latitude and longitude ordering.

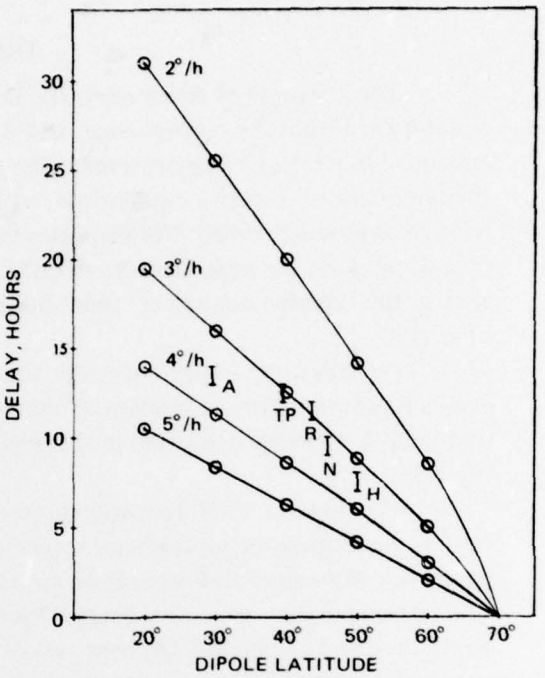

Figure A5. Onset time (shock front passage) versus latitude, with data of 8 March 1970 event for comparison.

SUMMARY

The "shock front" turbulent mixing model initially developed by Davies and investigated in this report can explain some of the phenomena exhibited in ionospheric storms. In general, ionospheric storms are found often to be localized in impact, with sudden decreases in the F_2-region density extending far down in latitude. The localized storm may be due to short and localized energetic heating in the auroral zone, which causes a disturbance propagating equatorward in a narrow "cone." The disturbance appears to propagate with a velocity of ~4°/h, which is much slower than the Alfven velocity (the velocity at which any plasma disturbance should propagate); therefore, the disturbance is expected to be propagating through the neutral atmosphere, perhaps in the form of gravity wave trains. That gravity waves are caused by auroral activity is well documented (Akasofu, 1968). In this report we have considered the possibility of developing a shock-front-like disturbance; this is expected because the earth's rotational motion causes the auroral oval (and polar cusp) to move at supersonic velocities relative to the earth's atmosphere. The model does describe accurately some of the events seen in the 8 March 1970 event documented by Klobuchar and others (1971).

BIBLIOGRAPHY

Akasofu, SI, "The development of the auroral substorm," Planet Space Sci, 12, 273, 1964

Akasofu, SI, "Polar and magnetospheric substorms," Springer Verlag, 1968

Akasofu, SI, "Magnetospheric substorms: a model," Solar Terrestrial Physics/1970, part III, p 131-151, Oxford Press, 1972

Akasofu, SI, The aurora and the magnetosphere, Chapman Memorial Lecture, Planet Space Sci, 22, 885, 1974

Akasofu, SI, "The solar wind – magnetosphere dynamo and the magnetospheric substorm," Planet Space Sci, 23, 817, 1975

Akasofu, SI, and Chapman, Solar Terrestrial Physics, Oxford Press, 1972

Akasofu, SI, and Kan, JR, "Some new thoughts on magnetospheric substorms," Radio Sci, 8, 1099, 1973

Akasofu, SI, and Snyder, AL, "Comments on the growth phase of magnetospheric substorms," J Geophys Res, 77, 6275, 1972

Akasofu, SI, and others, "Auroral substorms and the interplanetary magnetic field," J Geophys Res, 78, 7990, 1973

Axford, I, "Magnetospheric convection," Rev of Geophys, 7, 921, 1969

Banks, PM, and Nagy, AF, "Cyclonic disturbances and their consequences in the thermosphere," Geophys Res Letters, 1, 305, 1975

Davies, K, Ionospheric Radio Waves, Blaisdell Publishing Co, Walthrow, MA, 1965

Davies, K, "Studies of ionospheric storms using a simple model," J Geophys Res, 79, 605, 1974

Fukushima, N, "Polar magnetic substorms," Planet Space Sci, 20, 1443, 1972

Hirshberg, J, and Holzer, T, "Relationship between the interplanetary magnetic field and isolated substorms," J Geophys Res, 1975

Jones, KL, "Storm time variation of F2-layer electron concentration," J Atmos and Terr Phys, 33, 379, 1971

Kamide, Y, "Association of DP and DR fields with the interplanetary magnetic field variations," J Geophys Res, 70, 89, 1974

Kamide, Y, and others, "Weak and intense substorms," Planet Space Sci, 23, 579, 1975

Kane, RP, "Storm time variation of F2 region," Annls Geophys, 29, 25, 1973

Kane, RP, "Global evolution of the ionospheric electron content during some magnetic storms," J Atmos and Terr Phys, 37, 601, 1975

Klobuchar, JA, and others, "Ionospheric storm of March 8, 1970," J Geophys Res, 76, 6202, 1971

Lanzerotti, LJ, Cogger, LL, and Mendillo, M, "Latitude dependence of ionospheric total electron content: Observations during sudden commencement storms," J Geophys Res, 80, 1287, 1975

Matsushita, S, "A study of the morphology of ionospheric storms," J Geophys Res, 64, 305, 1959

McPherron, RL, "Substorm related changes in the geomagnetic tail: the growth phase," Planet Space Sci, 20, 1521, 1972

McPherron, RL, Russell, CT, and Aubry, MP, "Satellite studies of magnetospheric substorms on August 15, 1968, a phenomenological model for substorms," J Geophys Res, 78, 3131, 1973

Mendillo, M, "Ionospheric total electron content behavior during geomagnetic storms," Nature, 234, 23, 1971

Mendillo, M, and Klobuchar, J, An Atlas of the midlatitude F-region response to geomagnetic storms, AFCRL Technical Report 74-0065, February 1974

Obayashi, T, Research in Geophys, chapter 14, vol 1, MIT Press, Cambridge, 1964

Papagiannis, MD, Mendillo, DM, and Klobuchar, JA, "Simultaneous storm-time increases of the ionospheric total electron content and the geomagnetic field in the dusk sector," Planet Space Sci, 19, 503, 1971

Park, CG, "A morphological study of substorm-associated disturbances in the ionosphere," J Geophys Rev, 79, 2821, 1974

Patton, DE, and Cohen, ML, "A simple magnetic storm prediction model suitable for real-time frequency management," Raytheon report published at ARPA-OHD Tech Review, 17-18 March 1971

Prolss, GW, and Najita, K, "Magnetic storm associated changes in electron content at low latitudes," J Atmos Terr Phys, 37, 635, 1975

Richmond, AD, and Matsushita, S, "Thermospheric response to a magnetic substorm," J Geophys Res, 80, 2839, 1975

Rishbeth, H, and Hanson, WB, "A comment on plasma 'pileup' in the F-region," J Atmos and Terr Phys, 36, 703, 1974

Roederer, J, "Planetary plasmas and fields," Trans of American Geophys Union (EOS), 57, p 53, February 1975

Rush, CM, "Some effects of neutral wind changes on the low latitude F-region," J Atmos Terr Phys, 34, 1403, 1972

Russell, CT, and McPherron, RL, "The magnetotail and substorms," Space Sci Rev, 15, 205, 1973

Ruster, R, and Dudeney, JR, "The importance of the non-linear term in the equation of motion of the neutral atmosphere," J Atmos Terr Phys, 34, 1075, 1972

Schindler, K, "A theory of the substorm mechanism," J Geophys Res, 79, 2803, 1974

Svalgaard, L, "Geomagnetic responses to the solar wind and solar activity," Stanford University, Institute for Plasma Research, report 555, 1973

Yasuhara, F, Kamide, Y, and Akasofu, SI, "A model of the magnetospheric substorm," Planet Space Sci, 23, 575, 1975